NANOSYSTEMS:
PHYSICS, CHEMISTRY, MATHEMATICS

Perelmuter M.N. *Nanosystems:*
Phys. Chem. Math., 2022, **13** (4), 356–364.
http://nanojournal.ifmo.ru
DOI 10.17586/2220-8054-2022-13-4-356-364

Original article

Interface cracks bridged by nanofibers

Mikhail N. Perelmuter

Ishlinsky Institute for Problems in Mechanics RAS, Moscow, Russia

perelm@ipmnet.ru

PACS 46.25.Cc, 68.35.Np

ABSTRACT The model of different materials joint with bridged interface crack is considered. It is assumed that between the crack faces there are nanofibers constraining the crack opening. The size of the zone filled with nanofibers (the bridged zone) can be comparable to the whole crack length. The bond tractions depend on the crack opening at the bridged zone according to the prescribed nonlinear bond deformation law. The system of two singular integral-differential equations with Cauchy-type kernel is used for evaluation of bond tractions for the interface crack bridged by nanofibers. A phenomenological description of the bond deformation law in the crack bridged zone is used. Numerical experiments have been performed to analyze the influence of the bilinear bond deformation law parameters, the size of the crack bridged zone and also the magnitude of the external load on the convergence of the numerical iteration solution of the integral-differential equations system.

KEYWORDS bridged crack, nanofibers, nonlinear bonds deformation law, stress state, stress intensity factors.

ACKNOWLEDGEMENTS This work was supported by the Government program (contract AAAA-A17-117021310386-3).

FOR CITATION Perelmuter M.N. Interface cracks bridged by nanofibers. *Nanosystems: Phys. Chem. Math.*, 2022, **13** (4), 356–364.

1. Introduction

Models of a crack with interaction of its faces make it possible to combine the approaches of fracture mechanics and physics of strength in the analysis of crack growth. Zones of the crack faces interaction (fracture process zones) are usually adjacent to the crack tips. In these zones forces applied to the crack faces restrain the crack opening, [1]. There are two main versions of fracture process zone models depending on the stress singularity condition at the crack tip - cohesive and bridged (see reviews [2], [3]). If several physical mechanisms are involved in the processes of materials deformation and rupture then in such case, it is more effective to use the process zone models with the crack tips stresses singularity accounting. Such models (in the terminology of [3], these are bridged crack models) have been studied for cracks in homogeneous materials as two-dimensional problems [4–8] and as axisymmetic problems [9–11]. For interface cracks, the bridged crack model have been extended and developed for two-dimensional case in [12, 13] and for axisymmetic problems in [14].

In fracture mechanics, the crack bridging model is used to analyze fracture toughness and cracks growth assuming the bridged zone destruction as cracks advance. Application of the bridged crack model together with the crack growing criterion [15, 16] allows one to obtain dependencies of materials toughness and strength versus a crack length. The toughening effects of bonds is presented, mathematically, by bonds deformation law. The bonds deformation law for straight nanofibers was considered in [17–19] on the basis of shear-lag model. Straight nanofibers orientations influence on composite fracture toughness was considered in [20,21]. The effects of nanotubes curvature on bonds deformation law were analysed in [22,23]. The fracture toughness of oriented multi-wall carbon-nanotube-reinforced alumina composites was experimentally obtained and it was compared with results obtained by analytical and numerical models [24, 25]. Results confirm that the contribution to toughness from the nanotube bridging induced considerable nanoscale toughening.

In this paper, the interface crack bridged zone model is used with the following assumptions: 1) a zone of weakened bonds between materials is considered as an interfacial crack with distributed nonlinear spring-like bonds (nanofibers) between the crack faces (bridged zone, see Fig. 1); 2) distributed bridging tractions, which are functions of the crack opening, are imposed to the crack faces at the bridged zone, see Fig. 2; 3) materials ahead of the crack tips are considered as linearly-elastic; 4) ahead of crack tips, these materials are deformed together with the infinitely thin adhesion layer without loss of their continuity; 5) the total stress intensity factor (due to the action of the external loading and the bridging tractions) is not zero. Note that the last assumption defines the main difference between cohesive and bridged models. Bonding in the crack bridged zone reduces the stress intensity factors. This effect depends on the bridged zone length and bonds properties, but within the crack bridging model (in contrast to cohesive crack models) tractions are assumed to exist together with a stress singularity at the crack tip.

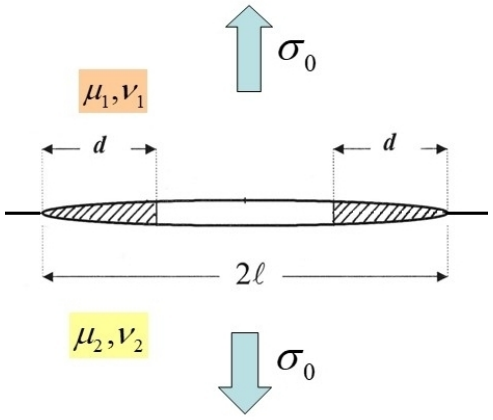

FIG. 1. Crack with two bridged zones at the materials interface

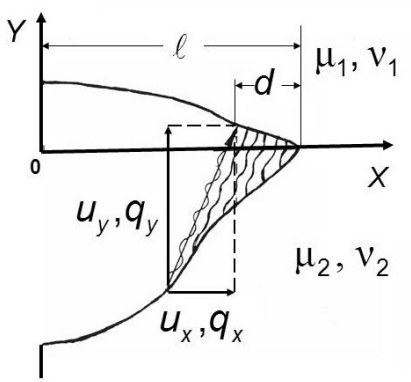

FIG. 2. Components of the crack opening $u_{x,y}$ and bonds tractions $q_{x,y}$ at the bridged zone

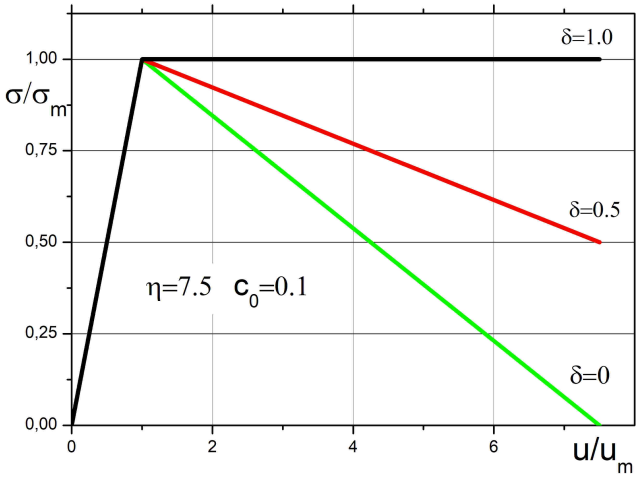

FIG. 3. Bilinear bonds deformation law, $u_m = 10^{-7}m$, $\sigma_m = 50$ MPa, $u_{cr} = \eta u_m$, softening parameter δ variation

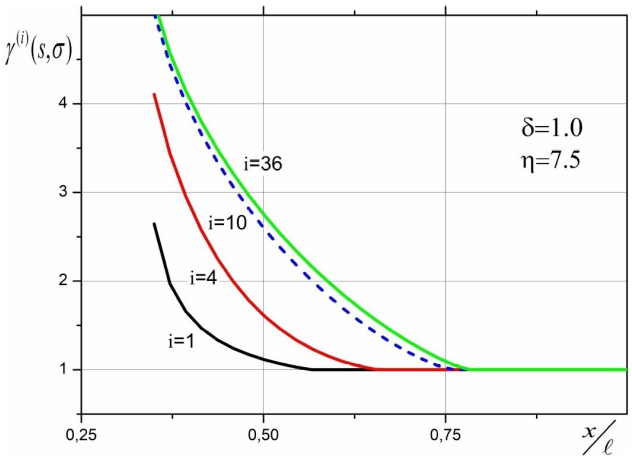

FIG. 4. Relative bond compliance over bridged zone length, $d/\ell = 0.65$, external load - $\sigma_0 = 40$ MPa

2. Statement of the problem

Let us consider the main statements of the interface bridged crack model proposed in [12]. Under external loads in bonds connecting the crack faces in the bridged zone (Fig. 2) tractions $Q(x)$ with normal $q_y(x)$ and tangential $q_x(x)$ components are arisen (even for loads normal to the crack line)

$$Q(x) = q_y(x) - iq_x(x), \quad i^2 = -1, \quad \sigma(x) = \sqrt{q_y^2(x) + q_x^2(x)}, \tag{1}$$

where $q_{y,x}(x)$ are the normal and shear components of the bonds tractions, respectively, $\sigma\,(x)$ is the bond stress vector modulus.

Normal and tangential stresses, numerically equal to $q_y(x)$ and $q_x(x)$, respectively, are applied to the crack faces at the bridged zone.

The crack opening, $u(x)$, at the bridged zones $\ell - d \le |x| < \ell$ is determined as follows

$$u(x) = u_y(x) - i\,u_x(x) = c_b(x,\sigma)(q_y(x) - iq_x(x)), \tag{2}$$

$$c_b(x,\sigma) = \varphi(x,\sigma)\frac{H}{E_b}, \quad u_b(x) = \sqrt{u_y^2(x) + u_x^2(x)}, \tag{3}$$

where $u_{y,x}(x)$ are the projections of the crack opening on the coordinate axes (Fig. 2), $c_b(x,\sigma)$ is the effective compliance of quasi-linear bonds depending on the bond position in the bridged zone and the bonds tension $\sigma(x)$, H is a linear scale related to the thickness of the intermediate layer adjacent to the interface, E_b is the effective elasticity modulus of the bond, $\varphi(x,\sigma)$ is dimensionless function which defines variation of bonds compliance over bridged zone and $u_b(x)$ is the modulus of the crack opening. Accounting the problem linearity, it is possible to write the crack opening $u(x)$ at the

bridged zone as follows

$$u(x) = u_\infty(x) - u_Q(x)\ , \tag{4}$$

where $u_\infty(x)$, $u_Q(x)$ are the crack opening caused by the external load σ_0 and bond tractions $Q(x)$ closing crack faces, respectively.

By using formulae (2)-(4), we can obtain a system of integral-differential equations relative to bonds tractions $q_{x,y}(x)$. Introduce the new variables, $s = x/\ell$, $q_{y,x}(s) = q_{y,x}(x)/\sigma_0$, and differentiate relation (4) with accounting relation (1)-(2) one obtains

$$c_0 \frac{\partial}{\partial s} \varphi(s,\sigma)\ [q_y(s) - i\, q_x(s)] + u'_Q(s) E_b = u'_\infty(s) E_b\ , \quad c_0 = \frac{H}{\ell}, \tag{5}$$

Here the right side of this relation is the given coordinate function and c_0 is the relative bond compliance.

The derivatives in relation (5) are defined as follows: the derivative of the crack opening under the action of homogeneous external loading $u'_\infty(s)$ is determined by the well-known solution presented in [26]; the derivative of the crack opening caused by bonds stress action $u'_Q(s)$ can be obtained starting from the representation for the derivatives of the opening crack under the action of arbitrary static loads on the crack faces. Following [12] and [13], one can obtain the system of two singular integral-differential equations (SIDE) relative to bonds tractions $q_y(s)$ and $q_x(s)$ in the form

$$T_{ij}(s,\sigma)\frac{df_j(s)}{ds} + W_{ij}(s,\sigma) f_j(s) + \varepsilon \int\limits_{1-d/\ell}^{1} G_{ij}(s,\xi) f_j(\xi) d\xi = Z_i(s);\ i,j = 1,2; \tag{6}$$

where $f_j(s)$ is unknown function depending on bond tractions $q_{x,y}(s)$ as follows

$$q_y(s) - i q_x(s) = (f_2(s) - i f_1(s))\sqrt{1-s}\left(\frac{1-s}{1+s}\right)^{-i\beta}, \tag{7}$$

and

$$\beta = \frac{\ln\ \alpha}{2\pi},\ \alpha = \frac{\mu_1 + \mu_2\kappa_1}{\mu_2 + \mu_1\kappa_2},\ \varepsilon = \frac{E_b}{2\pi c_0}\left(\frac{k_1+1}{\mu_1} + \frac{k_2+1}{\mu_2}\right), \tag{8}$$

In relations (8) $\kappa_{1,2} = 3 - 4\nu_{1,2}$ or $\kappa_{1,2} = (3-\nu_{1,2})/(1+\nu_{1,2})$ for plane strain and plane stress, respectively, $\nu_{1,2}$ and $\mu_{1,2}$ are Poisson's ratios and the shear modulus of jointed materials 1 and 2, ε is the main parameter affecting the SIDE solution, it includes the relative stiffness of bonds in the crack bridged zone and the mechanical properties of the both materials.

The singular kernel $G_{ij}(s,\xi)$ and the vector-column $Z_i(s)$ in equation (6) can be written as [13]

$$G_{ij}\,(s,\xi) = \frac{(1-\xi)\sqrt{1+\xi}}{(\xi^2 - s^2)\sqrt{1+s}}\begin{bmatrix} s & -\xi\cdot\Omega\,(s) \\ s\cdot\Omega\,(s) & \xi \end{bmatrix}, \quad \Omega\,(s) = \tan\left(\beta \ln\frac{1-s}{1+s}\right),$$

$$Z_i(s) = \frac{\pi\,\varepsilon}{2\cosh\,(\pi\beta)\sqrt{1+s}}\begin{bmatrix} 2\beta\cdot\,\Omega(s) - s \\ -2\beta - s\cdot\,\Omega(s) \end{bmatrix}.$$

The details of SIDE (6) derivation and the explicit relations for the coefficients of this equation $T_{ij}(s,\sigma)$, $W_{ij}(s,\sigma)$ (which depend on coordinates, properties of materials, function $\varphi(s,\sigma)$ and its derivatives with respect to s) are presented in [13].

3. Bonds deformation curves and numerical solution

To model the stress state in the crack bridged zone, it is convenient to present the nonlinear bond deformation law (the relationship between the crack opening and the bonds tractions) in a relatively simple analytical form, described by the minimum number of parameters, which can be experimentally obtained. As the first step simplification of bonds deformation law, one can rewrite it as follows

$$\sigma(u_b) = \begin{cases} \kappa_b(s) u_b(s), & 0 \le u_b(s) \le u_m \\ \Phi(u_b), & u_m < u_b(s) \le u_{cr}, \end{cases} \tag{9}$$

where the initial part of bonds deformation law is assumed as linear-elastic, it may depend on the bond position along the crack bridged zone ($s = x/\ell$), $\sigma(s)$ and $u_b(s)$ are defined by relations (2)-(3), $\kappa_b(s)$ is the bond stiffness and the slope of the elastic rising segment of the deformation law, u_m is the crack opening corresponding to transition from the linear-elastic to non-linear parts of the bond deformation law. The parameter u_m depends, in particular, on the mechanical and physical characteristics of bonds and the crack length.

For the numerical solution of equations (6), we use the iteration scheme which is similar to the well-known elastic steps method. At each iteration, equations (6) is solved by a collocation scheme with a piecewise-quadratic approximation of the unknown functions, see details in [13]. The method of variable elasticity parameters for solving equations (6) is

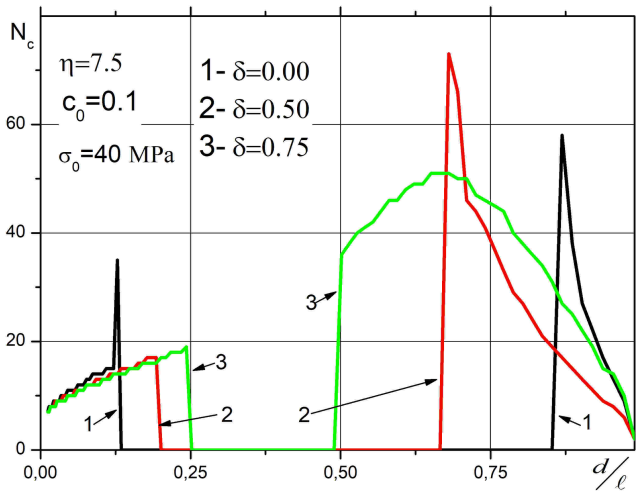

FIG. 5. Number of iterations until solution convergence versus crack bridged zone length, external load – $\sigma_0 = 40$ MPa

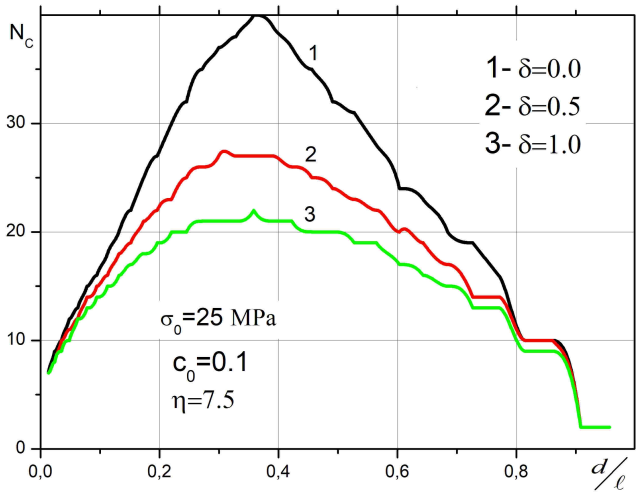

FIG. 6. Number of iterations until solution convergence versus crack bridged zone length, external load – $\sigma_0 = 25$ MPa

realized as the method of the tangential compliance with assumption that nonlinear part of the bond deformation law is given by the explicit relation. The first step of the iteration process consists of solving equations (6) for linear elastic bonds. Subsequent iterations are performed if, on the crack bridged zone part, $u(s) > u_m$. At each iteration, equations (6) are solved for quasi-elastic bonds with an effective compliance that is variable along the crack bridged zone and depends on the magnitude of the tractions vector modulus in the bonds obtained at the previous solution step. The effective compliance is calculated in a similar manner for the determination of the secant modulus in the variable elasticity parameters method. The process of successive approximations terminates when there is little difference in the bonds tractions that are obtained in two successive iterations. In the current version of the computer code, the termination of the solution is performed if the relative difference in two successive iterations is less then $\omega = 10^{-5}$.

The non-linear part of the bond deformation curve can be described as a monotonically decreasing or increasing function, the specific form of which depends on the type and characteristics of the bonds in the crack bridged zone. The decreasing non-linear part of the bond deformation curve corresponds to the weakening of bonds as the crack opening increases. The criterion of the limiting elongation of bonds assumes that bond rupture occurs when the limiting elongation of the bond, u_{cr}, is reached with the bond critical stress, σ_{cr}, corresponding to this bond elongation value. Depending on the type of bonds, the magnitude of σ_{cr} may also be zero. Note that the iteration process also terminates (before convergence is reached) if the crack opening on the bridged zone edge exceeds u_{cr}, which corresponds to the impossibility of static equilibrium of the bridged zone for the crack of given length. Two types of the non-linear polynomial decreasing parts of the bond deformation curve were proposed in [13]. It was assumed that the decreasing part of the bond deformation curve is a power-law function (convex and concave) passing through points with the coordinates (u_m, σ_m) and (u_{cr}, σ_{cr}) in the (u, σ) plane (here $\sigma_m = \kappa_b(s)u_m$ is the maximum stress corresponding to transition to non-linear part of the bond-deformation law). The bilinear law of bonds deformation is widely used as effective simplification of the general nonlinear deformation law [19, 27]. It can be written in our case as

$$\sigma(u_b) = \begin{cases} \kappa_b(s)u_b(s), & 0 \le u_b(s) \le u_m \\ \dfrac{\sigma_m}{(\eta-1)}\left[\left(\eta - \dfrac{u_b(s)}{u_m}\right) + \delta\left(\dfrac{u_b(s)}{u_m} - 1\right)\right], & u_m < u_b(s) \le u_{cr}, \end{cases} \tag{10}$$

where the following notations are used

$$\eta = \frac{u_{cr}}{u_m}, \qquad \delta = \frac{\sigma_{cr}}{\sigma_m}. \tag{11}$$

When $\sigma_{cr} < \sigma_m$ $(\delta < 1)$, the second dependence in (10) is decreasing (softening). When $\sigma_{cr} > \sigma_m$, it is the increasing one (linear hardening), and the ideal plasticity condition is satisfied when $\delta = 1$. Relative bond elongation before it breaks is defined by the parameter $\eta > 1$.

4. Convergence of iteration solution and bridged stresses

Consider a crack of length $2\ell = 10^{-3}m$ at the interface of half-planes of different materials (the junction of a metal (elastic modulus $E_1 = 135\,GPa$) and a hard reinforced polymer (elastic modulus $E_2 = 25\,GPa$) and Poisson's ratios of the materials $\nu_1 = \nu_2 = 0.35$) with two bridged zones of equal size, filled with bonds. It is assumed that the bond deformation law is a bilinear diagram. The initial elastic part of this diagram has the bond stiffness constant along of

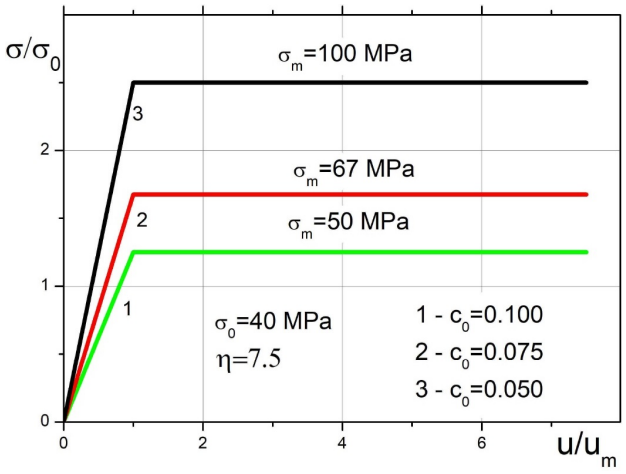

FIG. 7. Bilinear bonds deformation law, perfect plasticity ($\delta = 1$), $u_{cr} = \eta u_m$, variation of initial relative compliance c_0, external load – $\sigma_0 = 40$ MPa

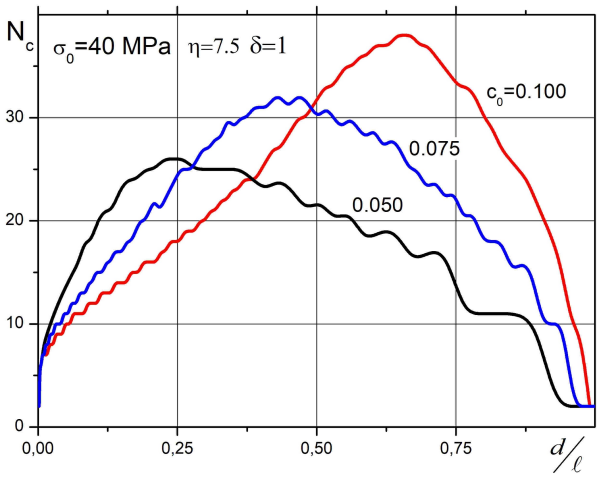

FIG. 8. Number of iterations until solution convergence versus crack bridged zone length, external load – $\sigma_0 = 40$ MPa, variation of initial relative compliance c_0

the bridged zone (see (3)) $\kappa_b = {c_b}^{-1} = E_b/H$, the elastic modulus of nanofibers is $E_b = E_2$ and $\varphi(s,\sigma) = 1$). The crack opening value for transition to the second part of the bond deformation law is assigned as $u_m = 10^{-7}m$. In the calculations, the size of the crack bridged zone is regarded as a free parameter, and the convergence of the iteration process and the stress distributions in the crack bridged zone are analysed for $0 < d \le \ell$.

We will obtain some parameters of the deformation law, expressing them in terms of the relative compliance of bonds c_0. The value of compliance c_b on the elastic part of the deformation diagram for the crack of length $2\ell = 10^{-3}m$ and with the elastic modulus of nanofibers $E_b = 25\,GPa$ can be written as

$$c_b = c_0 \frac{\ell}{E_b} = c_0 \frac{0.5 \cdot 10^{-3}}{25 \cdot 10^9} = 2c_0 \cdot 10^{-8}\text{m/MPa}.$$

According to (9) the maximum elastic stress admissible in bonds is

$$\sigma_m = u_m/c_b = 5/c_0\,\text{MPa}. \tag{12}$$

When $c_0 = 0.1$ (this value of the relative compliance corresponds to elastic deformation of bonds consisting of polymer molecules bundles or nanonfibers), we obtain the values $c_b = 2 \times 10^{-9}$ m/MPa and $\sigma_m = 50$ MPa. These parameters have been used to plot the graphs according to the relation (10) for different dishardening parameters δ (Fig. 3).

To illustrate the iterative solution of the SIDE for $\delta = 1, \eta = 7.5$, some results of calculations at the external load $\sigma_0 = 40$ MPa, and $d/\ell = 0.65$ are presented. The change in the relative bonds compliance along the crack bridged zone $\gamma^{(i)}(s,\sigma)$ is shown in Fig. 4 where

$$\gamma^{(i)}(s,\sigma) = c_b^{(i)}(s,\sigma)\frac{E_b}{H}, \quad s = \frac{x}{\ell}.$$

Here $\gamma^{(1)}(s,\sigma) = 1$ is the initial relative compliance of bonds at the first step of iteration solution. The solution convergence in this example is achieved in $N_c = 36$ iterations. The iterative process converges quite fast and after the 7th-8th iteration the solution parameters change slightly.

Changing the softening parameter in the range $0 \le \delta \le 1$ under constant external load significantly affects on the iteration process convergence.

Due to strong bonds stress concentration in the elastic solution [12], the minimum external load for which non-linear deformation of bonds will occur for $c_0 = 0.1$ is about $\sigma_0 = 11$ MPa [13]. It was numerically revealed that for bilinear dependence under the external load 11 MPa $\le \sigma_0 \le 40$ MPa and $0.9 \le \delta \le 1$, the iterative solution converges at any size of the crack bridged zone, and when parameter δ decreases, regions of solution divergence arise. Iterations number dependencies N_c until the solution convergence versus the crack bridged zone length under the external load $\sigma_0 = 40$ MPa , $\eta = 7.5$ and softening parameter values $\delta = 0.0;\ 0.5;\ 0.75$ is shown in Fig. 5. If $\delta = 0.0$, the divergence zone of the iterative solution occupies more than half of the crack length ($0.13 < d/\ell < 0.87$), for $\delta = 0.50$ the divergence zone is $0.19 < d/\ell < 0.68$ and for $\delta = 0.75$ the divergence zone decreases up to $0.25 < d/\ell < 0.50$. In all these cases of solution divergence, there is no static equilibrium state for the given external load and bonds deformation law. Decreasing the external load allows one to achieve the solution convergence at any values of the parameter δ. For the external load $\sigma_0 = 25$ MPa iterations number dependencies until solution convergence is achieved versus the crack bridged zone length, at variation of softening parameter δ is shown in Fig. 6. The maximum number of iterations depends significantly on the

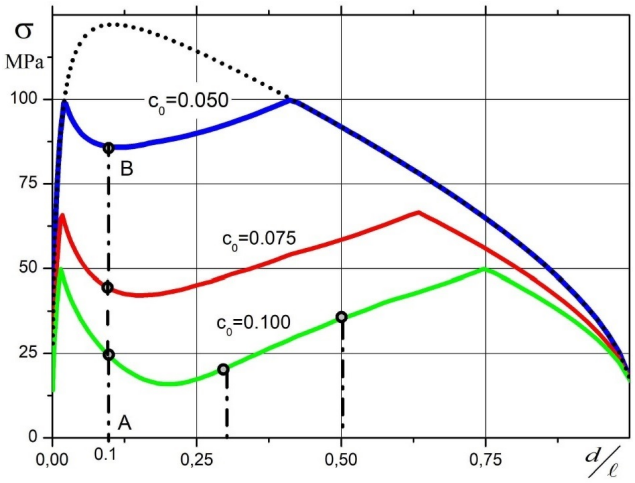

FIG. 9. Traction vector modulus at the crack bridged zone edge vs bridged zone length, $\eta = 2$, $\delta = 0.5$, external load – $\sigma_0 = 17.5$ MPa

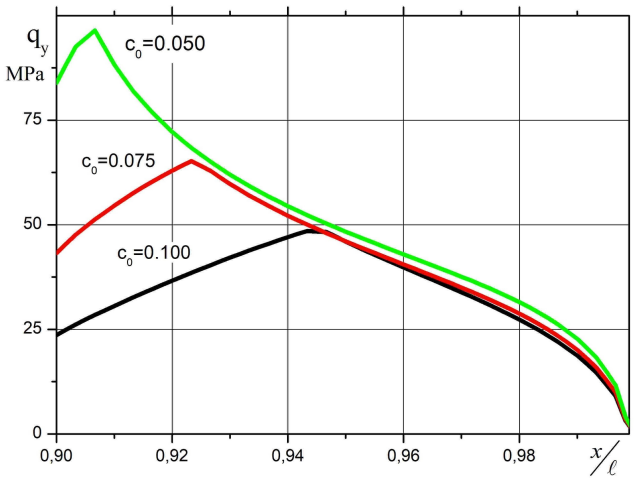

FIG. 10. Normal traction over bridged zone length, $d/\ell = 0.1$, $\eta = 2$, $\delta = 0.5$, external load – $\sigma_0 = 17.5$ MPa

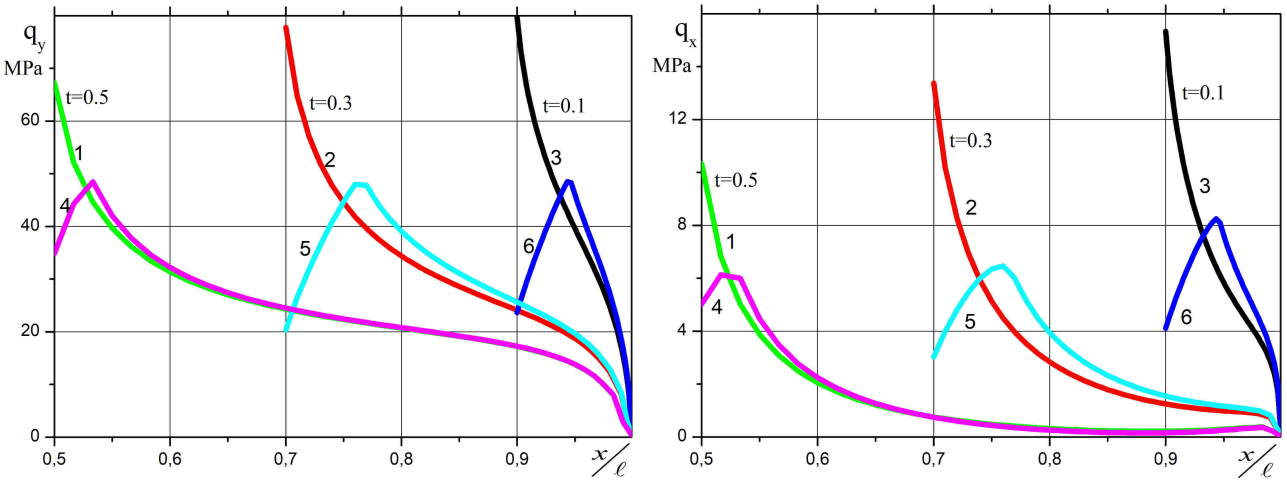

a) **b)**

FIG. 11. Normal **(a)** and shear **(b)** bond traction over bridged zone, $1, 2, 3$ – elastic solution, $4, 5, 6$ – nonlinear solution, $\eta = 2$, $\delta = 0.5$, external load - $\sigma_0 = 17.5$ MPa, $t = d/\ell$

softening parameter, and the position of this maximum keeps when parameter δ changes. The number of iterations for which convergence of the iterative solution process is achieved increases in proportion to the external load value.

Bonds deformation diagrams with different stiffness of the initial elastic part and with the next perfect plasticity part ($\delta = 1$) for the external load $\sigma_0 = 40$ MPa are shown in Fig. 7. As stiffness of the elastic part of this diagram increases then relative compliance of bonds decreases and the maximum stress corresponding to transition to the second part of the diagram increases ($\sigma_m = 67$ MPa and $\sigma_m = 100$ MPa, see (12)).

The maximum number iterations up to the solution convergence reduces with decreasing of bonds relative compliance in view of increasing the stress σ_m. The position of the iteration number maximum shifts towards the small sizes of the crack bridged zone with decreasing of bonds relative compliance (see Fig. 8) because the maximum elastic stress value at the trailing edge of the bridge also shifts to a small zone size, [12].

Decreasing of bonds relative compliance c_0 and keeping $u_m = const$ lead to reduction of crack bridged zone range covered by nonlinear deformation because together with compliance, the crack opening in the bridged zone also decreases in the elastic solution [12]. For relatively big external load, this zone reduction is weak (see Fig. 8), but when the external load decreases, the zone reduction is noticeable. The results for less load shown in Fig. 9–11 were also obtained for different bonds relative compliance but for external load $\sigma_0 = 17.5$ MPa and $\eta = 2$ and $\delta = 0.5$. The dependence of the traction vector module σ at the crack bridged zone edge versus the bridged zone relative size d/ℓ is given in Fig. 9. If the bonds deformation diagram with a dishardening branch is considered then the most significant traction redistribution occurs at the range of the bridged zone sizes d/ℓ close to the position of the bonds traction maximum in linear-elastic

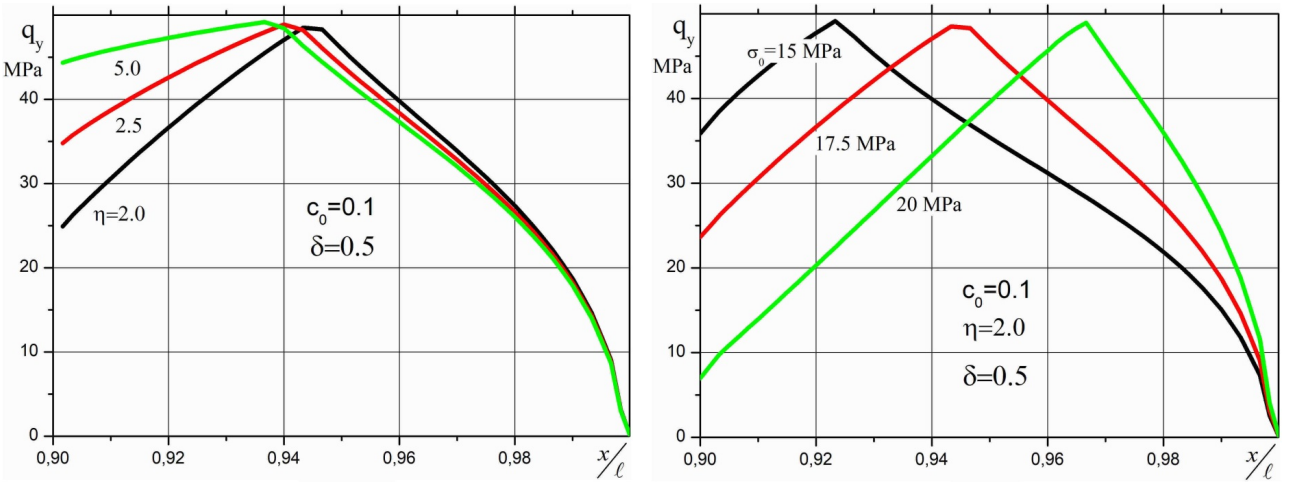

a) **b)**

FIG. 12. Normal bonds tractions over bridged zone, $d/\ell = 0.1$: **(a)** -external load - $\sigma_0 = 17.5$ MPa, variation of parameter η; **(b)** - variation of external load

solution, see the upper line in Fig. 9 which corresponds to linear-elastic solution. In Fig. 9 it can be noticeable seen the decreasing the zone of nonlinear deformation with the decreasing of the relative bond compliance. The effect of the relative bonds compliance variation on the zone of nonlinear deformation size is also illustrated by Fig. 10. At the specified external load ($\sigma_0 = 17.5$ MPa) and at the crack bridged zone length $d/\ell = 0.1$ (the position of this zone size is also marked in Fig. 9, line $A - B$), the size of the bonds nonlinear deformation zone increases if the relative bond compliance c_0 of the linear part of the deformation curve increases.

Distributions of the normal and tangent tractions at the external load $\sigma_0 = 17.5$ MPa, for the bonds deformation parameters of $\eta = 2$, $\delta = 0.5$ and $c_0 = 0.1$ are shown in Fig. 11 for $t = d/\ell = 0.1, 0.3, 0.5$. Stresses at the trailing edge of these bridged zones are shown in Fig. 9 by grey circles. For the given load the range of the crack bridged zones length, in which nonlinear deformation of the bonds is possible is $0.015 \le d/\ell \le 0.75$ (see Fig. 9). As the length of the crack bridged zone increases, the value of elastic stresses in the bonds decreases and, accordingly, a part of the crack bridged zone with nonlinear bonds deformation also decreases.

Changing the parameter $\eta = u_{cr}/u_m$ has a noticeable effect on the distribution of tractions in the region of bonds nonlinear deformation (see Fig. 12a). As $u_{cr}/u_m \to \infty$ than distribution of tractions in the region where $u(x) > u_m$ approaches to uniform $\sigma(x) \to \sigma_m$ since the convergence of iterative process is reached at $u \ll u_{cr}$. Increasing of the external load at fixed length of crack bridged zone and the prescribed bonds deformation curve leads to increasing of bonds nonlinear deformation region (see Fig. 12b).

The stress intensity factors (SIF) for bridged crack depend on the bridged zone length and the parameters of bonds deformation law. Having the distribution of bonds traction over the crack bridged zone, one can calculate the stresses ahead of the crack tip and the SIFs following to [12]:

$$K_{\rm I} + iK_{\rm II} = \lim_{\varrho \to 0} \sqrt{2\pi\varrho}\, \left(\sigma_{yy}(\varrho) + i\sigma_{xy}(\varrho)\right) \left(\frac{\varrho}{2\ell}\right)^{-i\beta}, \tag{13}$$

where $\sigma_{yy}(\varrho)$ and $\sigma_{xy}(\varrho)$ are the stresses ahead the crack tip caused by the external loads and by the bonds traction, ϱ represents the small distance to the crack tip.

The total SIFs due to external load and bonds tractions can be defined as follows

$$K_{\rm I} + iK_{\rm II} = \left(K_{\rm I}^{ext} + K_{\rm I}^{\rm int}(d)\right) + i\left(K_{\rm II}^{ext} + K_{\rm II}^{\rm int}(d)\right), \; K_b = \sqrt{K_I^2 + K_{II}^2}, \tag{14}$$

where $K_{I,II}^{ext}$ and $K_{I,II}^{int}(d)$ are the SIFs caused by the external loads and the bond tractions and K_b is the SIFs modulus.

On the basis of relationships for the stress distribution ahead the interface crack tip under arbitrary loads on the crack faces [28] and using statements (13)-(14), we can obtain the total SIFs for the interface straight bridged crack under the external tension load σ_0 [12]

$$K_{\rm I} + iK_{\rm II} = \sigma_0\sqrt{\pi\ell}\left[(1 + 2i\beta) - \frac{2\cosh(\pi\beta)}{\pi}\int\limits_{1-d/\ell}^{1} \frac{(p_y(\xi) + i\xi p_x(\xi))}{\sqrt{1-\xi^2}}\, d\xi\right], \tag{15}$$

where $p_{x,y}$ are dimensionless amplitudes of bonds traction $q_{x,y}(s)$

$$p_y(\xi) - ip_x(\xi) = (q_y(\xi) - iq_x(\xi))\left(\frac{1-\xi}{1+\xi}\right)^{i\beta}.$$

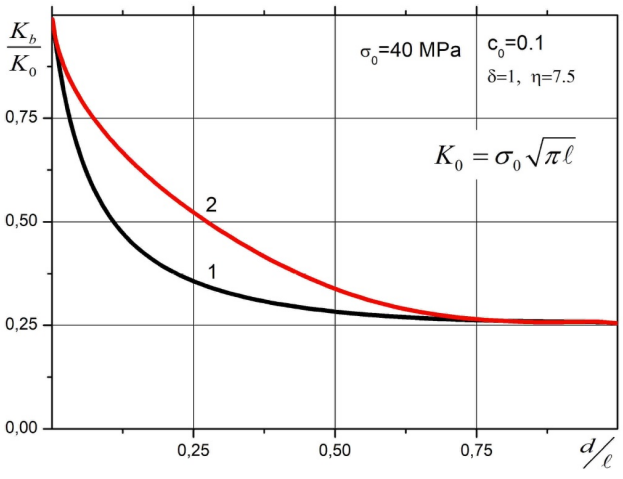

FIG. 13. Relative SIF versus the crack bridged zone length: 1 – linear-elastic bonds; 2 – bilinear bonds deformation law

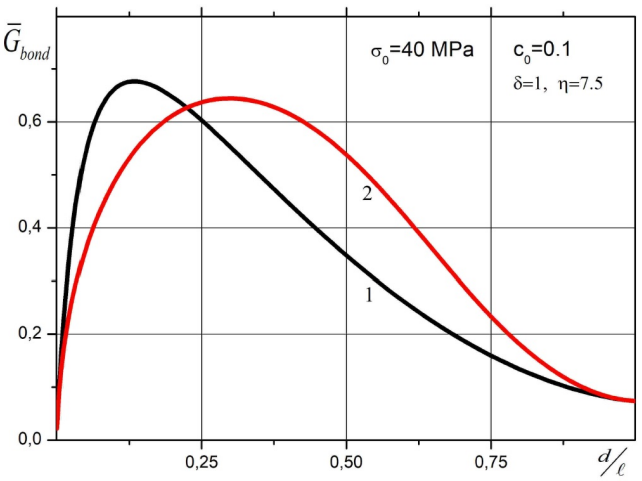

FIG. 14. The rates of deformation energy absorption by bonds: 1 – linear-elastic bonds; 2 – bilinear bonds deformation law

Let's consider the effect of the bond deformation law on the level of the stress intensity factors. Decreasing the softening parameter δ of the bond deformation law leads to reducing of the stress level in the crack bridged zone bonds and, therefore, the SIF increases. Increasing the bond compliance of the linear part bond deformation law leads to nonlinear deformation region enlargement. For example, in Fig. 13, the dependence of the SIF module versus the crack bridged zone length for $\sigma_0 = 40$ MPa and $c_0 = 0.1$ is shown. The nonlinear deformation zone and the degree of softening of the bonds increase with increasing of the bonds compliance.

Two energy characteristics of interfacial bridged cracks are used in bridged cracks growth criterion [15]:

1) the deformation energy release rate associated with the crack tip stress intensity factors (15) is as follows

$$G_{\rm tip}(d,\ell) = \left(\frac{\kappa_1+1}{\mu_1} + \frac{\kappa_2+1}{\mu_2}\right)\frac{K_b^2}{16\,\cosh^2(\pi\beta)}, \tag{16}$$

2) the rate of the energy absorbtion by bonds associated with the energy necessary to create a unit of new surface of the bridged zone is as follows

$$G_{\rm bond}(d,\ell) = \int\limits_{\ell-d}^{\ell}\left(\frac{\partial\, u_y(x)}{\partial\,\ell}q_y(u) + \frac{\partial\, u_x(x)}{\partial\,\ell}q_x(u)\right)dx, \quad \bar{G}_{bond} = \frac{G_{bond}\,(d,\ell)}{G_{tip}\,(0,\ell)}, \tag{17}$$

where $\bar{G}_{bond}$ is the dimensionless energy parameter, $G_{tip}(0,\ell)$ is the energy release rate for a crack without bridged zone.

The effect of the bonds deformation law on the bridged crack energy characteristic $\bar{G}_{bond}$ is shown in Fig. 13. For linear-elastic bonds in the crack bridged zone, the rate of energy consumption by bonds reaches a maximum value at a certain size of the bridged zone. Changing the law of bonds deformation results in a change in this energy parameter in the whole non-linear deformation zone, which in this case covers the entire range of the crack bridged zones, as well as a shift in the position of the maximum of this function to larger value of the size of the bridged zone.

5. Conclusion

Parametric description of nonlinear bonds deformation law in the crack bridged zone as the bilinear diagram taking into account sections of softening makes it possible to evaluate effects of basic characteristics of deformation curves on the numerical solution convergence, to investigate tractions distribution over bonds in the crack bridged zone, and also evaluate effect of softening on energy parameters of bridged cracks.

The results obtained can be useful (despite the limited possibility of transferring the solution of non-linear problems to other scales) in the development of methods for solving similar problems for bridged cracks by finite and boundary element methods.

The model of bridged crack at the materials interface allows one to analyze bonds tractions distribution for different laws of bonds deformation, to evaluate the crack limit equilibrium taking into account the kinematic and energy conditions of fracture, see [15]. The model can be used at different fracture scales and allows one to analyse the process of fracture of adhesive compounds and composites from unified point of view, including the stages of defect onset, crack formation and growth at the nano-, micro- and macro-scales.

References

[1] Barenblatt G.I. The mathematical theory of equilibrium cracks in brittle fracture. In H.L. Dryden, Th. von Karman, G. Kuerti, F.H. van den Dungen, and L. Howarth, editors, *Advances in Applied Mechanics*, 1962, **7**, P. 55–129.

[2] Bao G. and Suo Z. Remarks on Crack-Bridging Concepts. *Applied Mechanics Reviews*, 1992, **45**(8), P. 355–366.

[3] Cox B.N. and Marshall D.B. Concepts for bridged cracks in fracture and fatigue. *Acta Metallurgica et Materialia*, 1994, **42**(2), P. 341–363.

[4] Walton J.R. and Weitsman Y. Deformations and stress intensities due to a craze in an extended elastic material. *Journal of Applied Mechanics*, 1984, **51**(1), P. 84–92.

[5] Weitsman Y. Nonlinear analysis of crazes. *ASME. Journal of Applied Mechanics*, 1986, **53**, P. 97–103.

[6] Rose L.R.F. Crack reinforcement by distributed springs. *Journal of the Mechanics and Physics of Solids*, 1987, **35**(4), P. 383–405.

[7] Budiansky B., Amazigo J.C. and Evans A.G. Small-scale crack bridging and the fracture toughness of particulate-reinforced ceramics. *Journal of the Mechanics and Physics of Solids*, 1988, **36**(2), P. 167–187.

[8] Willis J.R. Asymptotic analysis of crack bridging by ductile fibres. *Composites*, 1993, **24**(2), P. 93–97.

[9] Willis J.R. and Movchan N.V. Penny-shaped crack bridged by fibres. *Quarterly of Applied Mathematics*, 1998, **56**(2), P. 327–40.

[10] Grekov M.A. and Morozov N.F. Equilibrium cracks in composites reinforced with unidirectional fibres. *Journal of Applied Mathematics and Mechanics*, 2006, **70**(6), P. 945–955.

[11] Selvadurai A.P.S. Bridged defects in continuously and discretely reinforced solids. *Journal of Engineering Mathematics*, 2015, **95**(1), P. 359–80.

[12] Goldstein R. and Perelmuter M. Modeling of bonding at an interface crack. *International Journal of Fracture*, 1999, **99**, P. 53–79.

[13] Perelmuter M.N. An interface crack with non-linear bonds in a bridged zone. *Journal of Applied Mathematics and Mechanics*, 2011, **75**(1), P. 106–118.

[14] Perelmuter M. Stress analysis of composites with interfacial bridged cracks and damaged zones. *Journal of Physics: Conference Series*, 2022, **2231**, P. 012021–1–012021–7.

[15] Perelmuter M.N. A criterion for the growth of cracks with bonds in the end zone. *Journal of Applied Mathematics and Mechanics*, 2007, **71**(1), P. 137–153.

[16] Perelmuter M.N. Analysis of crack resistance of interfaces between materials. *Mechanics of Solids*, 2020, **55**(4), P. 536–551.

[17] Perelmuter M.N. Mechanical modelling of nanotube-polymer adhesion. *NANOSYSTEMS: PHYSICS, CHEMISTRY, MATHEMATICS*, 2011, **2**(2), P. 119–125.

[18] Wang J., Tong L., and Karihaloo B.L. A bridging law and its application to the analysis of toughness of carbon nanotube-reinforced composites and pull-out of fibres grafted with nanotubes. *Archive of Applied Mechanics*, 2016, **86**(1), P. 361–73.

[19] Hu Y.-G., Ma Y.L., Hu C.P., Lu X.Y. and Gu S.T. Analysis of stress transfer in short fiber-reinforced composites with a partial damage interface by a shear-lag model. *Mechanics of Materials*, 2021, **160**, P. 103966.

[20] Mirjalili V. and Hubert P. Modelling of the carbon nanotube bridging effect on the toughening of polymers and experimental verification. *Composites Science and Technology*, 2010, **70**(10), P. 1537–1543.

[21] Meng Q., Li B., Li T. and Feng X-Q. Effects of nanofiber orientations on the fracture toughness of cellulose nanopaper. *Engineering Fracture Mechanics*, 2018, **194**, P. 350–361.

[22] Chen X., Beyerlein I.J. and Brinson L.C. Bridged crack models for the toughness of composites reinforced with curved nanotubes. *Journal of the Mechanics and Physics of Solids*, 2011, **59**(9), P. 1938–1952.

[23] Budarapu P.R., Kumar S., Prusty B.G., and Paggi M. Stress transfer through the interphase in curved-fiber pullout tests of nanocomposites. *Composites Part B: Engineering*, 2019, **165**, P. 417–434.

[24] Xia Z., Riester L., Curtin W.A., Li H., Sheldon B.W., Liang J., ChangB. and Xu J.M. Direct observation of toughening mechanisms in carbon nanotube ceramic matrix composites. *Acta Materialia*, 2004, **52**(4), P. 931–944.

[25] Xia Z., Curtin W.A. and Sheldon B.W. Fracture toughness of highly ordered carbon nanotube/alumina nanocomposites. *Journal of Engineering Materials and Technology*, 2004, **126**(3), P. 238–244.

[26] England A.H. A crack between dissimilar media. *ASME. Journal of Applied Mechanics*, 1965, **32**(2), P. 400–402.

[27] Alfano G. and Crisfield M.A. Finite element interface models for the delamination analysis of laminated composites: mechanical and computational issues. *International Journal for Numerical Methods in Engineering*, 2001, **50**(7), P. 1701–1736.

[28] Perelmuter M.N. Bridged crack – opening outside of the bridged zone and stresses at the material interface. *Vestnik I. Yakovlev Chuvach State Pedagogical University. Series: Mechanics of a limit state*, 2020, **2**(44), P. 69–77.

Submitted 9 August 2022; revised 17 August 2022; accepted 18 August 2022

Information about the authors:

Mikhail N. Perelmuter – Ishlinsky Institute for Problems in Mechanics RAS, Vernadsky avenue 101-1, Moscow, 119526, Russia; perelm@ipmnet.ru

Conflict of interest: the author declare no conflict of interest.